

AN EXPERIMENTAL INVESTIGATION OF HUB DRAG CHARACTERISTICS ON COAXIAL ROTOR AIRCRAFT

Min Tang, MingQi Huang, YongDong Yang, Dong Li

Key Laboratory of Rotorcraft Aerodynamics, China Aerodynamics Research and Development Center, Mianyang City, 621000, China

Abstract

A full-scale wind tunnel tests have been conducted to research the hub drag characteristics of combine coaxial rotor aircraft and better understand the aerodynamic interaction between hub and fairings. A hub and fairing drag test was conducted to obtain quantitative drag measurements on multiple fairing geometries, and to get insight into the effect of rotation and the presence of blade stub. There were four interchangeable mid-shaft fairings designed, i.e., optimized fairings F1, F2 based on airfoil and optimized fairing F3, plus a bare shaft(S) for reference. The effect on the hub drag of varying angle of attack, Mach number were investigated. Principal results were that the Mach number had a greater influence on the drag of hub, and the best fairing configuration reduced the drag of coaxial rotor hub by 37%. The test also provided validation data for computational fluid dynamics (CFD), and aerodynamic characteristics for design.

NOTATION

S	reference area, m^2
a	speed of sound, m/sec
CD	drag coefficient, D/qS
D	drag, N
CxS	drag area, D/q , m^2
Ma	Mach number, V/a
N	speed of rotation, rpm
q	dynamic pressure, $1/2 \rho V^2$
V	wind velocity, m/sec
α	angle of attack, deg
β	angle of sideslip, deg
ρ	air density, kg/m^3

INTRODUCTION

For conventional helicopters with a single main rotor, the drag of rotor hub is typically about 30% of the total rotorcraft drag and is higher for dual-rotor helicopters [1][2]. Especially for the coaxial rigid rotor combinational high-speed rotorcraft (figure 1) it was found that about 50% of the total aircraft drag was from the rotor hub assembly [3][4]. At high speeds forward flight, about 45% of the engine power to overcome the drag of the hub, it has greatly limited the flight performance of such helicopters. A key enabler to success of coaxial rotor aircraft is rotor hub drag reduction.

One method of reducing the drag of coaxial rotor hub is to enclose it in a streamlined fairing that rotates with hub. References 5 and 6-11 present data obtained in wind tunnel tests of various hub fairing configurations. These data include a wide range of Mach numbers, and angle of attack. To data, there have not been any

reports that evaluate the effect of coaxial rotor on the drag-reduction characteristics of a hub fairings.



Figure 1 S-97 Raider flight test

A series of full-scale wind tunnel tests have been conducted at China Aerodynamics Research and Development Center (CARD C) to research the hub drag characteristics of coaxial rotor, and to investigate several new hub drag reduction configurations. A photograph of full-scale model of coaxial rotor hub installed in CARD C $\Phi 3.2m$ wind tunnel is presented in fig 2.



Fig 2 hubs wind tunnel test in CARD C

One objective of this wind tunnel test was to examine the effects on the coaxial rotor hub drag of variations in angle of attack, Mach number, hub rotation, and blade stub. Another motive was to obtain quantitative drag measurements, to get insight into the effect of different hub fairing configurations.

1. Experimental Procedures

1.1. Description of wind tunnel and Balances

The $\Phi 3.2\text{m}$ Wing Tunnel at Low Speed Aerodynamic Research Institute of CARDC was used for this test. This is an opened/closed-throat, single-return tunnel with a speed capability extending to 145m/sec. It is located in the China MianYang in the China Aerodynamics Research and Development Center (see figure 3), where subsonic, transonic, supersonic and hypersonic facilities are also available.

Model forces and moments were measured by a six-component external mechanical balance. The drag measurement accuracy is 5N. The principal test velocities in the test of the full-scale model extended from 20m/sec to 70m/sec. All of the data in this paper are presented in the form of drag areas ranges from 0.441 to 0.447 m^2 .



Figure 3 China Aerodynamics Research and Development Center (MianYang, China)

Full-scale rotor-hub model forces and moments were measured by a six-component external balance. The drag balance had an accuracy of 5N. The test velocities in the full-scale test extended from 20 to 120 m/s. Results in this paper are presented in the form of drag areas, $C_x S = D/q$ [12].

1.2. Test facility and transmission

The test facility consists of a power unit, a support assembly and a transmission system. The Coaxial rotor hub system was mounted on the transmission assembly and powered by a single 120kw motor system. The transmission system reversed the lower hub rotation directly, while ensured that both upper and lower hub remain

synchronized, spinning at the same speed. The six-component external balance were mounted between the transmission system and support assembly.

1.3. Model description

The full-scale hub model of the coaxial rotor, shown in figure 4, had a main rotor pylon mounted on the support assembly that connected to the wind tunnel yaw table. The hub components included pylon fairing, lower hub, shaft fairing, and upper hub. The lower hub was mounted on the transmission system, it could rotate or not. Above it was the sail fairing, which had a lot of pressure taps. The upper/lower hub could be tested non-spinning without blade stubs, or it could be rotated with or without the stubs.

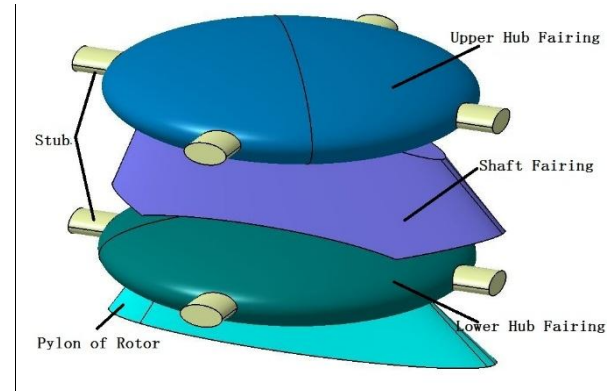


Figure 4 full-scale coaxial rotor hub model

There had three interchangeable sail fairings designed for getting insight into the effect of reduction drag, and a bare shaft for reference (figure 5). The upper and lower hub fairing were both elliptical shape and both of them were 1 meter diameter (figure 6). The main rotor pylon was built on the transmission support that mounted on the external balance.

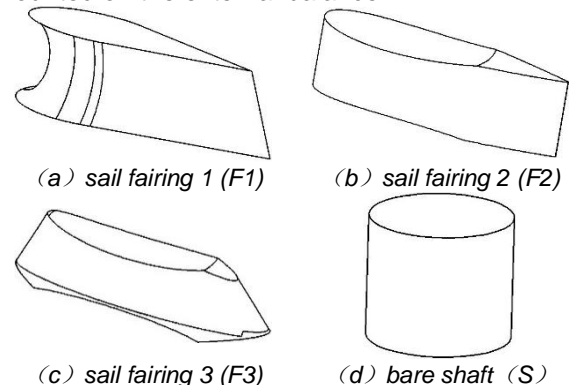


Figure 5 sail fairing model comparison

Both the upper and lower hub fairings had four stub blades which could be install or not, as shown in figure 6. When hub was not spinning, the stubs were at $\pm 45/90\text{deg}$ azimuth.

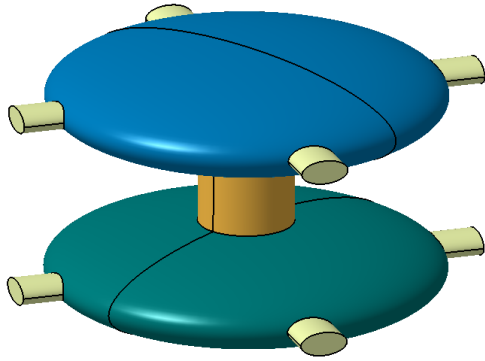


Figure 6 hub fairing model (H)

The down surface of upper hub fairing and up surface of lower hub fairing had a lot of steady pressure taps mounted equidistant from the two rotor hub radial direction. The airfoil sail fairing also had 30 steady pressure taps from the hub rotor planes on each side. An additional pressure tap was placed at the trailing edge.

These model were primarily constructed using selective laser sintering additive manufacturing from aluminium. The pylon was solid selective laser sintering nylon.

1.4. Test conditions

Table 1 lists the tunnel flow conditions and the model parameter ranged for the test.

Table 1 Test conditions and parameter

wind tunnel velocity	20~70m/sec
hub rotation speed	0,200,280rpm
angle of attack (α)	-4°,0°,+4°
angle of side slip (β)	-10°, -5°, 0°, +5°, +10°

The characteristic length was the diameter of hub model, which was 1m. The test was conducted at atmospheric stagnation pressure. The full-scale test covered a speed range extending to 70m/sec. The angle of attack was varied between -4deg and +4deg in test. Hub fairings angle of side slip sweeps were performed from -10° to +10°.

The blockage of the hub firings at $\alpha=0^\circ$ was approximately 3%. Blockage corrections was not made to the tunnel dynamic pressure values.

2. Results and Discussion

2.1. Effect of angle of attack and side slip on drag

Figure 7 presents the relationship between angle of attack and total hub assembly drag area as measured in the full-scale wind tunnel test. The data were obtained at a velocity of 50m/sec with the hub rotating. The configuration with middle rotor shaft fairing (F3) was tested which the hub

model had blade stubs or not. Figure 7 shown that the drag area increments caused by changed in the hub configuration were essentially independent of the angle of attack.

Figure 8 shown the relationship between the sideslip angle and drag area of coaxial rotor hub fairings. The data obtained at $Ma=0.177$ and $N=200rpm$. The plots shown that the drag area increments caused by changed in the hub configuration were also essentially independent of the angle of side slip. Therefore, all subsequent wind tunnel test data presented in this article will be at zero angle of attack and sideslip.

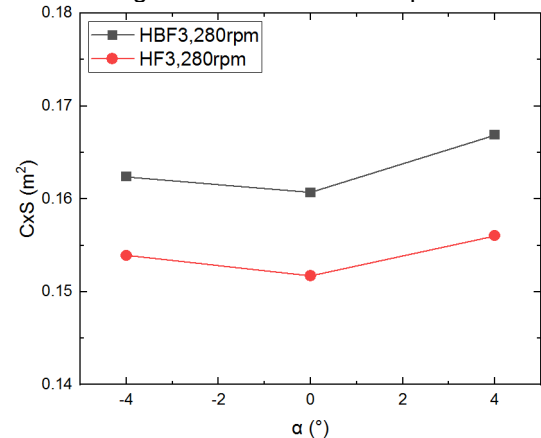


Figure 7 Effect of angle of attack on drag area ($N=280rpm$, $Ma=0.147$)

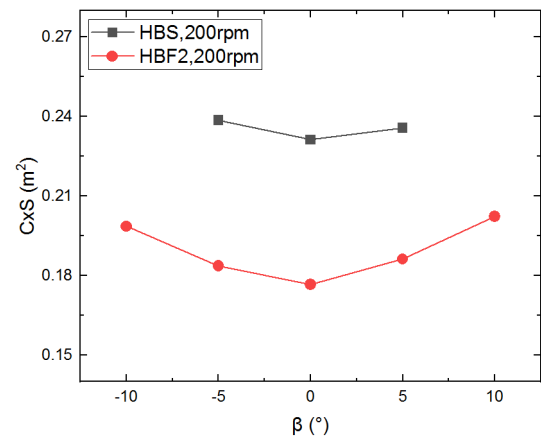


Figure 8 Effect of angle of sideslip on drag area ($Ma=0.177$)

2.2. Effect of Mach Number on drag

The full-scale wind tunnel test was conducted at atmospheric stagnation pressure. Therefore, the Mach number and Reynolds number changed simultaneously as the wind velocity was increased.

Figure 9 presented the effect of the Mach number on the drag of the coaxial rotor hub as measured in the full-scale wind tunnel test with stub blades and hubs rotation. The drag area of HBS and HBF1 hub configurations were not affected by the variation of Mach number. These data shown that for non-compressible flow of

subsonic sound, increases in Mach number do not change drag area of hub fairings.

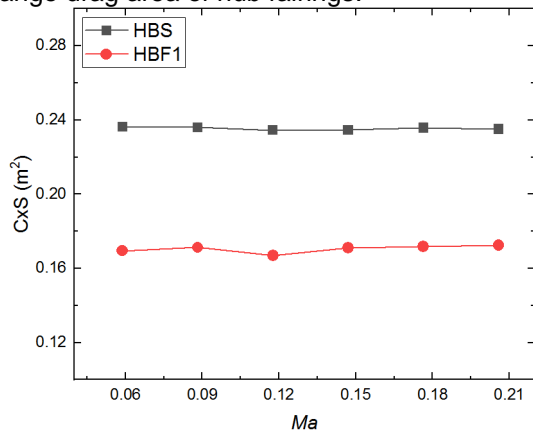


Figure 9 Effect of Mach number on drag area (N=200rpm)

2.3. Effect of hub rotation on drag

Figure 10 presented the effect of the hubs rotation on the drag of the coaxial rotor hub as measured in the full-scale wind tunnel test with stub blades. The plot presented that the drag area of coaxial rotor hubs with rotation had a little change compared to the hubs stationary. When the stub blades azimuth angle was 45deg, the drag area with the hubs stationary was slightly larger than the hubs rotating. To the contrary, the drag area with stub blades azimuth was 90deg minus the drag area with hubs rotating. It could be seen from fig.10 that hubs rotation did not have a significantly effect on the drag area of the faired hubs configurations (HBS).

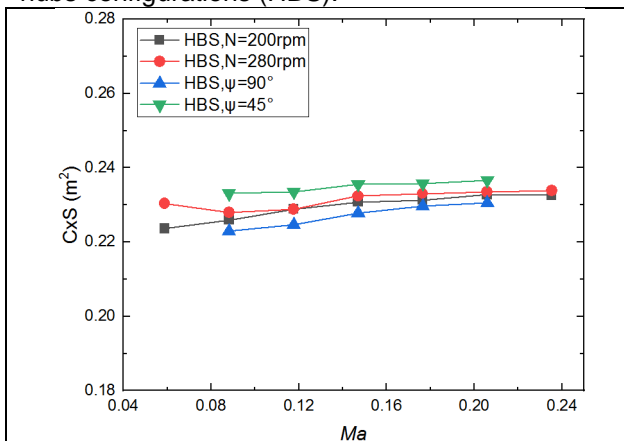


Figure 10 Effect of hub rotation on drag area

2.4. Effect of hub configuration on drag

Figure 11 presented the drag area results from the full-scale wind tunnel test with the hubs rotating at the highest Mach number of the test. The data noted that the lowest drag area hub configuration had about 37% less drag than the configuration with hub fairing and bare middle rotor shaft.

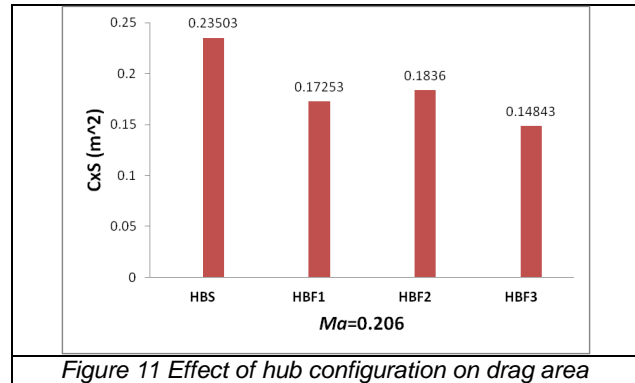


Figure 11 Effect of hub configuration on drag area

The HS configuration had the highest drag area than other configurations before the correction for middle rotor shaft fairing was applied. The reason that the middle rotor shaft increased the drag area was that the interconnecting shaft made the upper surface of lower hub fairing and lower surface of upper hub fairing had a V-shaped flow separation zone.

The HF3 configuration had the lowest drag area than other fairings because the F3 fairing extended trailing-edge and leading-edge compared with F1 and F2 fairing and reduced the size of the V-shaped separation zone.

Conclusions

Aerodynamic measurements of a full-scale coaxial rotor hub assembly obtained in the China Aerodynamics Research and Development Center's Φ 3.2m wind tunnel demonstrated the drag characteristics of hub drag reduction fairings. The following specific conclusions were reached.

1. Drag increments attributable to hub configuration changes were essentially independent of the angle of attack over an angle of attack range of -4deg to +4deg.

2. Drag increments attributable to hub configuration changes were essentially independent of the angle of side slip over an angle of side slip range of -10deg to +10deg.

3. When the hubs rotation, the drag area of the hub fairing (F1) and bare shaft configuration did not increase with increasing Mach number over a Mach number of range 0 to 0.3.

4. The drag area of faired rotor hub configurations on coaxial rotor hub was not significantly affected by hub rotation. There had slightly different between 90deg and 45deg azimuth with hubs stationary.

5. The lowest drag hub fairing configuration reduced the drag area of the bare shaft configuration by 37%. This was achieved with an optimized middle shaft fairing and with the minimum V-shaped flow separated zone.

References

- [1] Keys, C., and Wiesner, R. Guidelines for Reducing Helicopter Parasite Drag. Journal of the American Helicopter Society. 1975(20): 31-40.
- [2] Keys, C.N., and Rosenstein, H. Summary of rotor hub drag data NASA TR NASA CR-152080, 1978.
- [3] Ashish Bagai. Aerodynamic design of the X2 Technology Demonstrator Main Rotor Blade. Proceedings of 64th Annual Forum of the American Helicopter Society. 2008.
- [4] Brian E. Wake, Ebru Hagen, Stuart S. Assessment of Helicopter Hub Drag Prediction with an Unstructured Flow Solver. Proceedings of 65th Annual Forum of the American Helicopter Society. 2009.
- [5] Bertolotti, F, et al., Rotor Hub Fairing System for a Counter-Rotating Coaxial Rotor System. US Patent 7530787 B2, 2009.
- [6] Young Larry A, Graham, David R. Experimental Investigation of Rotorcraft Hub and Shaft Fairing Drag[C]. AIAA 4th Applied Aerodynamics Conference.1986.
- [7] Young Larry A, Graham, David R, Stroub Robert H. Reduction of Hub and Pylon Fairing Drag[C]. 43rd Annual Forum and Technology Display of the American Helicopter Society.1987.
- [8] Balch, D.T. and Weiner, S. 1/5 Scale ABC Hub Fairing Drag Test-Final Report[R]. Sikorsky Engineering Report. NASA2-10215.1980.
- [9] Bertolotti F P, Scott M W, Wake B E. e.t. Rotor Hub Fairing System for a Counter Rotating Coaxial Rotor System.US Patent 7 .2007.
- [10] Sheehy, T.W. and Clark, D.R., 'A method for predicting helicopter hub drag' TR-75-48,U.S.Army Air Mobility Research and Development Laboratory , Jan. 1976.
- [11] Logan, A.H. , Prouty, R,W, and Clark, D.R., 'Wind Tunnel Tests of large-and Small -scale rotor hubs and pylons,' TR-80-D-21,U.S.Army Aviation Research and Development Command , Apr. 1981.
- [12] D.M. Martin, R.W. Mort, L.A. Young, and P.K. Squires. , 'Experimental Investigation of Advanced Hub and Pylon Fairing Configurations to reduce Helicopter Drag ' NASA-TM-4540, Sep. 1993.